


RESEARCH ARTICLE

Optogenetic astrocyte activation evokes BOLD fMRI response with oxygen consumption without neuronal activity modulation

Norio Takata^{1,2}  | Yuki Sugiura³ | Keitaro Yoshida¹ | Miwako Koizumi¹ |
 Nishida Hiroshi¹ | Kurara Honda³ | Ryutaro Yano⁴ | Yuji Komaki² | Ko Matsui⁵ |
 Makoto Suematsu³ | Masaru Mimura¹ | Hideyuki Okano^{4,6} | Kenji F. Tanaka¹

¹Department of Neuropsychiatry, Keio University School of Medicine, 35 Shinanomachi, Shinjuku, Tokyo, 160-8582, Japan

²Central Institute for Experimental Animals (CIEA), 3-25-12, Tonomachi, Kawasaki, Kanagawa, 210-0821, Japan

³Department of Biochemistry, Keio University School of Medicine, 35 Shinanomachi, Shinjuku, Tokyo, 160-8582, Japan

⁴Department of Physiology, Keio University School of Medicine, 35 Shinanomachi, Shinjuku, Tokyo, 160-8582, Japan

⁵Super-network Brain Physiology, Graduate School of Life Sciences, Tohoku University, Sendai, Miyagi, 980-8575, Japan

⁶Laboratory for Marmoset Neural Architecture, RIKEN Brain Science Institute, Wako, Saitama, 351-0198, Japan

Correspondence

Norio Takata and Kenji F. Tanaka,
 Department of Neuropsychiatry, Keio
 University School of Medicine, 35
 Shinanomachi, Shinjuku, Tokyo, 160-8582,
 Japan.

Email: takata.norio@keio.jp and
 kftanaka@keio.jp

Funding information

Takeda Science Foundation; JSPS
 KAKENHI, Grant Numbers: 25430011,
 25115726, 15KT0111, 16H01620,
 16K07032, 24111551, 26290021, and
 16H06145; Brain/MINDS and the Strategic
 Research Program for Brain Sciences
 (SRPBS) from the Ministry of Education,
 Culture, Sports, Science, and Technology of
 Japan (MEXT); Japan Agency for Medical
 Research and Development (AMED)

Abstract

Functional magnetic resonance imaging (fMRI) based on the blood oxygenation level-dependent (BOLD) signal has been used to infer sites of neuronal activation in the brain. A recent study demonstrated, however, unexpected BOLD signal generation without neuronal excitation, which led us to hypothesize the presence of another cellular source for BOLD signal generation. Collective assessment of optogenetic activation of astrocytes or neurons, fMRI in awake mice, electrophysiological measurements, and histochemical detection of neuronal activation, coherently suggested astrocytes as another cellular source. Unexpectedly, astrocyte-evoked BOLD signal accompanied oxygen consumption without modulation of neuronal activity. Imaging mass spectrometry of brain sections identified synthesis of acetyl-carnitine via oxidative glucose metabolism at the site of astrocyte-, but not neuron-evoked BOLD signal. Our data provide causal evidence that astrocytic activation alone is able to evoke BOLD signal response, which may lead to reconsideration of current interpretation of BOLD signal as a marker of neuronal activation.

KEYWORDS

astrocytes, BOLD, fMRI, imaging mass spectrometry, optogenetics

1 | INTRODUCTION

Blood oxygenation level-dependent (BOLD) functional magnetic resonance imaging (fMRI) is a fundamental imaging tool in basic and clinical investigations of human brain activity (Ogawa, Lee, Kay, & Tank, 1990). The BOLD signal is not a direct measurement of neuronal activity; instead, the signal is influenced by cerebral blood flow (CBF), cerebral blood volume (CBV), and the cerebral metabolic rate of oxygen consumption (Ogawa, Menon, Kim, & Ugurbil, 1998; Shen, Ren, & Duong, 2008). Despite the above caveats, the BOLD signal has been widely

used as a surrogate marker of neuronal activation, because accumulating evidence has demonstrated a close correlation between BOLD signal response and electrophysiological activation of neurons following sensory stimulation (Logothetis, Pauls, Augath, Trinath, & Oeltermann, 2001; Niessing et al., 2005). Recent optogenetic fMRI (ofMRI) studies have further confirmed the correlation (Kahn et al., 2013; Lee et al., 2010; Takata et al., 2015). However, the cellular mechanisms of BOLD signal generation have not been fully elucidated (Ekstrom, 2010; Vanzetta & Sloviter, 2010). It is reported that coupling between BOLD and electrophysiological signal in visual cortex of behaving monkeys is



context dependent (Maier et al., 2008). Furthermore, unexpected BOLD signal generation is found without activation of local neurons in the visual cortex of monkeys performing a fixation-on-off task (Sirotnin & Das, 2009).

Astrocytes are also considered to participate in BOLD signal generation (Haydon & Carmignoto, 2006; Otsu et al., 2015; Schummers, Yu, & Sur, 2008; Takano et al., 2006), but in a passive way that just couples neuronal activity to the hemodynamic response to fulfill metabolic demand of neurons (Petzold & Murthy, 2011; Raichle & Mintun, 2006). A study that combined BOLD fMRI and fiber-optic calcium (Ca^{2+}) recording in the cortex of anesthetized rats during electrical paw stimulation reported a correlation between prolonged BOLD signal components and Ca^{2+} surge in astrocytes, and their modeling suggested involvement of astrocytes in a late component of the BOLD response (Schulz et al., 2012). However, direct investigation of causal relationship between astrocyte activation and BOLD signal generation seems difficult to examine in the study, because sensory stimulation inevitably activates neurons in addition to astrocytes. Moreover, a recent study reported intact BOLD signal response upon hindpaw stimulation of anesthetized inositol 1,4,5-triphosphate receptor type 2 knock-out ($\text{IP}_3\text{R2-KO}$) mice, which lack large cytosolic Ca^{2+} surges in astrocytes, suggesting a minor role of astrocytic Ca^{2+} activity in BOLD signal generation (Jego, Pacheco-Torres, Araque, & Canals, 2014) (but see (Srinivasan et al., 2015; Stobart et al., 2016) that demonstrate preserved Ca^{2+} dynamics in astrocytes of $\text{IP}_3\text{R2-KO}$ mice, and (Mishra et al., 2016) that shows multiple sources of calcium signals in astrocytes). Note that most of these studies were performed under anesthesia, which could affect neurovascular coupling, energy metabolism, and BOLD signal generation (Masamoto & Kanno, 2012; Sokoloff et al., 1977).

This study aimed to investigate a causal relationship between astrocyte activity and BOLD signal generation using ofMRI in awake transgenic mice, whose cortical neurons or astrocytes express channelrhodopsin-2 (ChR2) (Tanaka et al., 2012). Optical activation of either neurons or astrocytes by light illumination through intact skull evoked a BOLD signal response in the cortex. Oxygen consumption upon stimulation of either neurons or astrocytes was suggested by experiments of ofMRI in the presence of a vasodilator. Unexpectedly, optical activation of astrocytes did not modulate neuronal activity, which was confirmed with *in situ* hybridization for *c-fos* mRNA and *in vivo* electrophysiology. Metabolic underpinnings of the oxygen consumption was investigated with metabolite imaging of brain sections using imaging mass spectrometry (IMS). Activation of astrocytes, but not neurons, augmented synthesis of acetyl-carnitine (AC) from glucose, which consumed oxygen. Collectively, our findings demonstrate unexpected active role of astrocytes in BOLD signal generation.

2 | MATERIALS AND METHODS

2.1 | fMRI in awake mice

We have elaborated fMRI in awake mice using a high signal-to-noise ratio cryogenic MRI detector, CryoProbe (Yoshida et al., 2016).

Confounding effects of anesthetics during fMRI in awake mice were avoided because anesthesia is not necessary with this protocol to place awake mice in an animal bed of MRI.

2.2 | *In vivo* multichannel extracellular recordings

Extracellular recording was performed as described previously (Takata et al., 2015). A 16-channel, linear silicon probe was inserted through a craniotomy (Φ 0.5 mm; AP -3.0 mm, ML -2.0 mm) for recording from the cortex, which corresponds to the site of global peak of BOLD signal response upon optogenetic astrocyte activation (Figure 2c).

2.3 | IMS with FMW-assisted brain fixation for $^{13}\text{C}_6$ -glucose metabolic pathway tracing

Two-dimensional imaging of metabolites in the brain slices by combining IMS, focused microwave (FMW), and ^{13}C -isotope was reported previously (Sugiura, Honda, Kajimura, & Suematsu, 2014; Sugiura, Taguchi, & Setou, 2011). To trace the metabolic fate of glucose, $^{13}\text{C}_6$ -glucose was injected intraperitoneally. Fifteen minutes later (Sugiura et al., 2014), optogenetic stimulation of the left cortex through the intact skull was performed. Thirty seconds later, mice were euthanized by FMW-irradiation for 0.96 s on the brain (Sugiura, Honda, & Suematsu, 2015). Matrix-assisted laser desorption ionization (MALDI)-IMS was performed on thin sections of the brain. See Supporting Information Materials and Methods for more details.

3 | RESULTS

3.1 | Transcranial illumination of the cortex of awake mice that express ChR2(C128S) in neurons or astrocytes

Double transgenic animals that express ChR2(C128S), a step-function opsin-type variant of ChR2 (Berndt, Yizhar, Gunaydin, Hegemann, & Deisseroth, 2009), were generated by crossing a tetO-ChR2(C128S)-YFP line with a cell-type specific-tTA line (Tanaka et al., 2012); hereafter, we refer to *Chrm4-tTA::tetO-ChR2(C128S)-YFP* and *Mlc1-tTA::tetO-ChR2(C128S)-YFP* double transgenic lines as Neuron-ChR2 and Astrocyte-ChR2, respectively. For gene manipulation strategies to generate transgenic mice, see Supporting Information Figure S1. Expression of ChR2(C128S)-EYFP was observed in the cortex and sub-cortical brain structures of both Neuron- and Astrocyte-ChR2 mice (Figure 1a, d). Double immunostaining for NeuN (neuron marker) and YFP (ChR2-marker) showed high expression levels of ChR2(C128S) at neuronal somas in layer IV and at dendrites in layer II/III of the cortex of Neuron-ChR2 mice (Figure 1b,c). In Astrocyte-ChR2 mice, almost uniform expression of ChR2(C128S) was observed throughout the cortical layers (Figure 1e). The enlarged view of the staining reveals the expression pattern of ChR2(C128S) with fine laminar morphology that is characteristic of astrocytes (Figure 1f). Moreover, we have shown co-expression of ChR2(C128S) and GLAST, an astrocyte specific glutamate transporter, in the brain of Astrocyte-ChR2 mice (Tanaka et al., 2012), further confirming astrocytic expression of ChR2(C128S). Expression of

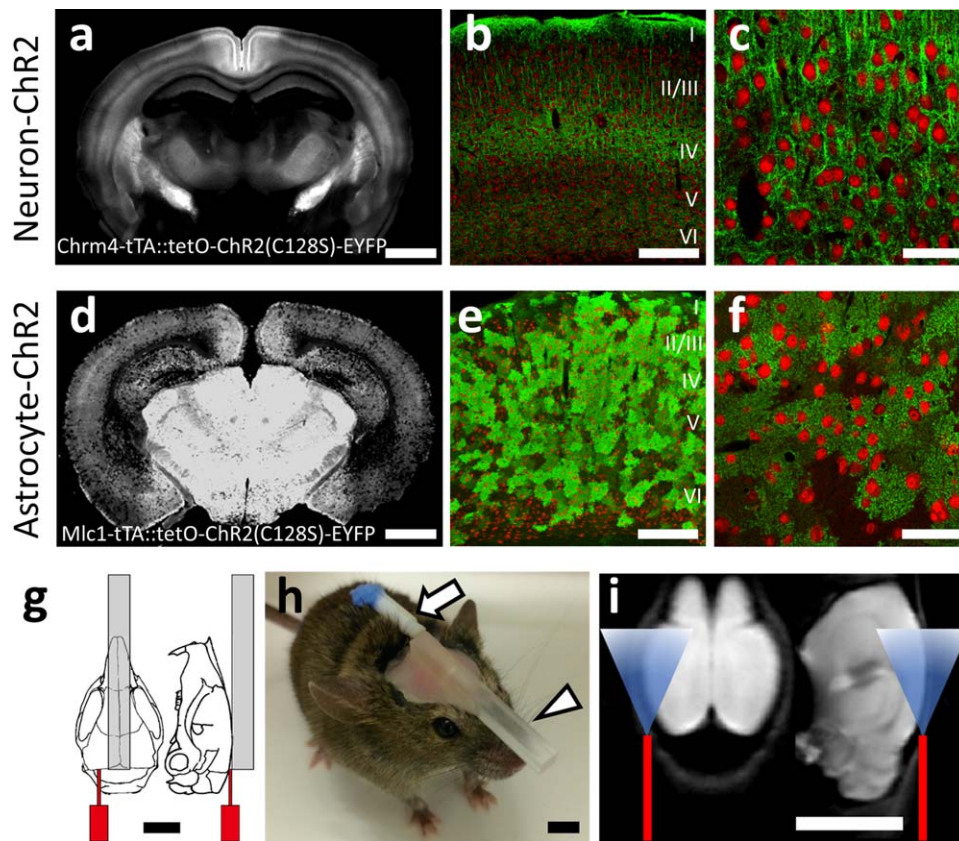


FIGURE 1 Transgenic mice that express ChR2(C128S)-EYFP at neurons or astrocytes. (a and d) Immunostaining against YFP (ChR2-marker) on coronal sections of the brain from Neuron- (a) and Astrocyte-ChR2 mice (d). (b and e) Double-immunostaining for NeuN (neuron marker, red) and YFP (green) of coronal sections of the brain from Neuron- (b) and Astrocyte-ChR2 mice (e). (c and f) Higher magnification images of cortical layer IV of Neuron- or Astrocyte-ChR2 mice. (g) Schematic drawings of attachment of a headbar (gray) and an optic fiber with a cannula (red) on the intact skull. A headbar was used for cranial fixation during ofMRI in awake mice. (h) A photograph of a transgenic mouse with an attached headbar (arrow head) and a fiber optic cannula (arrow). (i) Estimated area of illumination (pale blue) by an optic fiber (red), drawn over a horizontal (left) and a sagittal (right) brain section of an anatomical MRI image. Scale bar: a and d, 3 mm; b and e, 200 μ m; c and f, 50 μ m; g, h, and i, 5 mm [Color figure can be viewed at wileyonlinelibrary.com]

ChR2(C128S) across a wide cortical area in these transgenic mice lines allows transcranial manipulation of neuronal or astrocytic activity because ChR2(C128S) has higher sensitivity than conventional ChR2 (Mattis et al., 2012).

To perform light illumination through the intact skull of awake mice during fMRI experiments, a skull-holder and an optic fiber were attached horizontally on the skull (Yoshida et al., 2016). fMRI on awake mice is advantageous to avoid the confounding effects of anesthetics on neuronal and astrocytic activity (Greenberg, Houweling, & Kerr, 2008; Thrane et al., 2012). The tip of an optic fiber was positioned on the intact skull over the left visual cortex (Figure 1g-i).

3.2 | Optogenetic stimulation of astrocytes as well as neurons evokes BOLD signal response

We investigated whether transcranial photo-activation of neurons or astrocytes was able to induce a BOLD signal response using Neuron- or Astrocyte-ChR2 mice, respectively. Transcranial manipulation is desirable to avoid inserting an optic fiber into the brain, which may result in “reactive astrocytes” with distinct physiological characteristics

(Aguado, Espinosa-Parrilla, Carmona, & Soriano, 2002). We applied a pair of blue and yellow lights with 30 s separation, which kept a cation channel of ChR2(C128S) open for 30 s. This pair of lights was repeated 3 times at an interval of 2 min. The duration of each light was 0.5 and 5.0 s for Neuron- and Astrocyte-ChR2 mice, respectively. We employed longer illumination in Astrocyte-ChR2 mice because we speculated that effect of optogenetic stimulation was smaller in astrocytes, considering that astrocytic membrane resistance is lower than neurons.

We found that transcranial optogenetic stimulation of either neurons or astrocytes could evoke a BOLD signal response in the cortex (Figure 2a,c). The response was observed dominantly in the left cortex, which was ipsilateral to the site of light illumination. The most significant BOLD signal response was located within the cortex of Neuron- and Astrocyte-ChR2 mice (arrows in Figure 2a,c). Subcortical BOLD signal response may reflect direct photo-activation, based on our measurements of ofMRI using a triple transgenic mouse whose astrocytes express ChR2(C128S) except in the cortex (see Supporting Information Results and Figure S2a-d). In addition, light illumination for optogenetic stimulation seemed not enough to evoke BOLD signal response

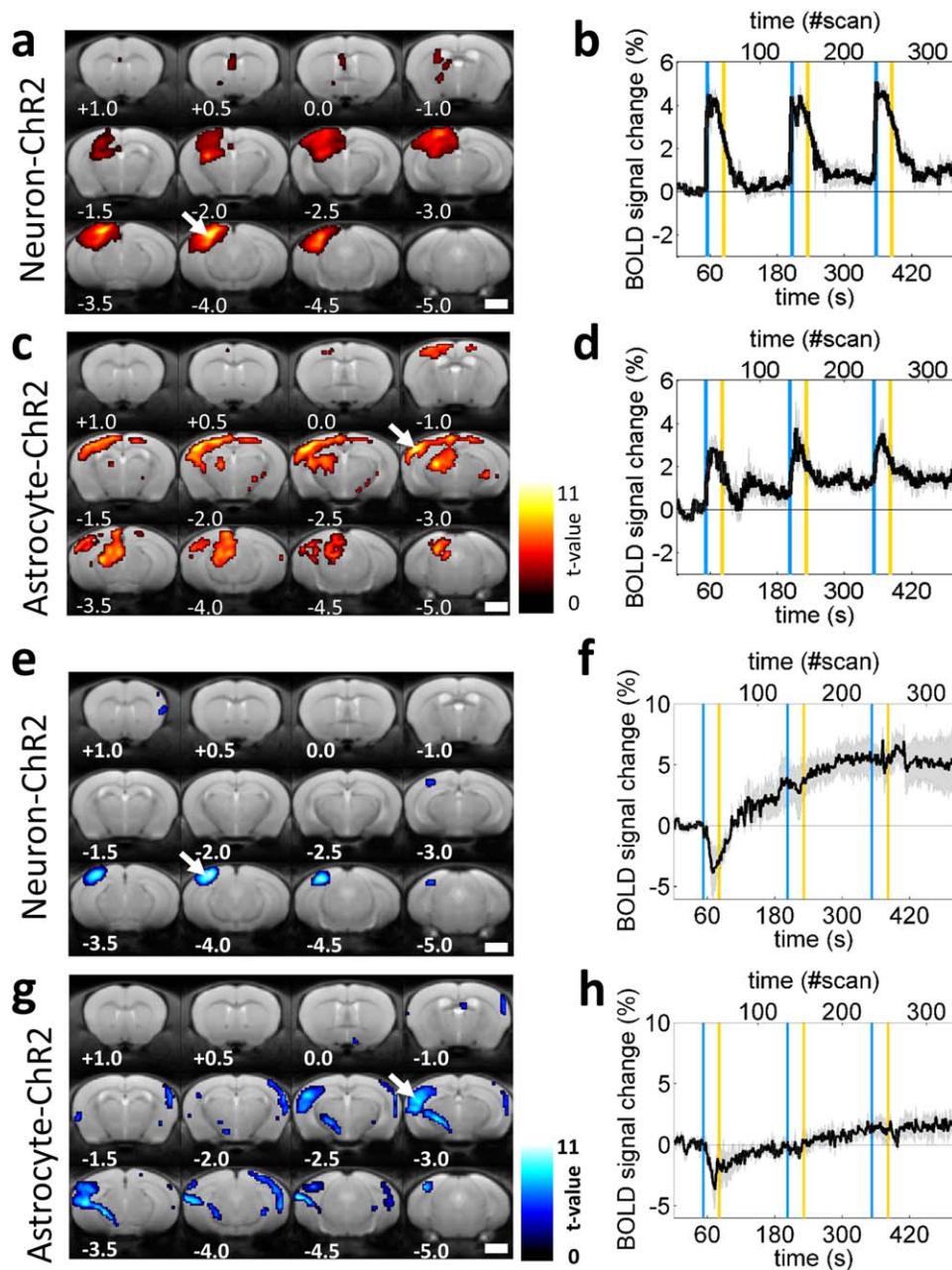


FIGURE 2 Transcranial optogenetic stimulation of neurons or astrocytes evoked BOLD signal response with oxygen consumption. (a and c) Activation t maps overlaid on structural MRI images showing spatial distribution of positive BOLD response upon optogenetic activation of cortical neurons (a) or astrocytes (c) from $n = 13$ Neuron- or 9 Astrocyte-ChR2 mice, respectively. Illumination was applied on the left side of the skull (left side in the figure). Values at the lower left indicate anterior-posterior (AP) distance from bregma in mm. Color bar indicates t values. Arrows at AP -4.0 and -3.0 mm in (a) and (c), respectively, indicate approximate position of a global peak of t values, which were used for locations of ROIs for BOLD time courses. (b and d) Time-course of BOLD signal fluctuation upon optogenetic activation of neurons (b) or astrocytes (d). Blue and yellow vertical lines show timing of illumination for each color. Note that ChR2 (C128S), a step function opsin with the closing time constant (τ) of 106 s, was kept open even after cessation of blue illumination until yellow illumination. The x-axis at the top shows the scan number of fMRI measurements. Gray shading indicates the SEM. (e–h) The same as (a–d), but in the presence of a vasodilator, SNP, from $n = 3$ Neuron- or 3 Astrocyte-ChR2 mice, respectively, showing negative BOLD response that indicates oxygen consumption upon optogenetic activation of neurons (f) or astrocytes (h). Scale bar: a, c, e, and g, 2 mm [Color figure can be viewed at wileyonlinelibrary.com]

through visual stimulation nor brain-tissue heating (see Supporting Information Results and Figure S3a,b). Further, ofMRI using *anesthetized* Astrocyte-ChR2 mice and open field test suggested that behavioral state-change, which may cause widespread astrocyte excitation in the brain, seemed not to contaminate BOLD signal fluctuation upon

optogenetic stimulation of astrocytes (see Supporting Information Results and Figures S2e,f and S4).

We compared temporal dynamics of BOLD signal fluctuations at the site of the most significant response upon optogenetic stimulation of Neuron- or Astrocyte-ChR2 mice, respectively (arrows in Figure 2a,

c). A BOLD signal response could be evoked repeatedly in both Neuron- and Astrocyte-ChR2 mice (Figure 2b,d). Peak amplitudes of the response during the first stimulation period, that is, 30-s period between a pair of blue and yellow vertical lines (Figure 2b,d), were significantly higher for Neuron- than Astrocyte-ChR2 mice ($6.1\% \pm 0.4\%$ vs. $4.7\% \pm 0.5\%$, $p = .03$, $n = 12$ and 9 animals for Neuron- and Astrocyte-ChR2 mice, respectively; two-sample t test). The magnitude of the BOLD signal response was dependent on the light intensities (Supporting Information Figure S3c,d).

3.3 | Oxygen consumption is elicited by optogenetic stimulation of either astrocytes or neurons

Because BOLD signal has been considered to reflect augmentation of the metabolic demand of neurons (Heeger & Ress, 2002), we addressed whether astrocyte-evoked BOLD signal response resulted in oxygen consumption. We performed ofMRI after injection of a nitric oxide-releasing vasodilator, sodium nitroprusside (SNP), so that oxygen consumption could be detected as negative deflection of the BOLD signal (Nagaoka et al., 2006).

Neuronal activation by optogenetic stimulation using Neuron-ChR2 mice in the presence of SNP resulted in a negative BOLD response (Figure 2e,f), which was in good accordance with previous studies (Nagaoka et al., 2006; Tsurugizawa, Ciobanu, & Le Bihan, 2013). The location of the most significant negative BOLD signal was similar to that of the positive BOLD response in ofMRI experiments without SNP (compare arrows in Figure 2a,e). The negative deflection of the BOLD signal occurred only once, followed by a gradual increase that exceeded baseline (Figure 2f).

Astrocyte activation by optogenetic stimulation using Astrocyte-ChR2 mice in the presence of SNP also resulted in a negative BOLD response (Figure 2g,h), which suggests that activation of astrocytes results in oxygen consumption. The location of the most significant negative BOLD signal was comparable to that of the positive BOLD response in ofMRI experiments without SNP (compare arrows in Figure 2c,g). Negative deflection of the BOLD response was observed only once to the first optogenetic stimulation of astrocytes (Figure 2h), which was similar to the result in Neuron-ChR2 mice (Figure 2f), although the gradual increase of the BOLD signal after the first optogenetic stimulation was not as clear as that in Neuron-ChR2 mice.

It's not clear in this study why negative deflection was hardly induced by the second and the third illumination on Neuron- or Astrocyte-ChR2 mice. BOLD signal is assumed to reflect increase of (a) blood volume, (b) blood flow, and (c) oxygenation in the blood (Shen et al., 2008). Considering that SNP suppresses the first two factors, gradual increase of BOLD signals might indicate physiological response to suppress oxygen consumption in the brain in the presence of SNP after the first optical stimulation. This might explain the absence of negative BOLD response upon the second and the third illumination.

3.4 | Neuronal activation is not observed by optogenetic stimulation of astrocytes

Because BOLD signal is used as a marker of neuronal activation, we examined the modulation of neuronal activity upon optogenetic stimulation of Neuron- or Astrocyte-ChR2 mice. We first performed *in situ* hybridization for *c-fos* mRNA, a neuronal activity marker, to obtain the spatial distribution of neuronal activation. Animals were perfused 30 min after optogenetic stimulation, and then post-fixed, sliced, and stained for *c-fos* mRNA.

Neuronal activation of Neuron-ChR2 mice increased *c-fos* mRNA staining in the ipsilateral cortex to the site of light illumination (Figure 3a), which is consistent with previous reports (Stark, Davies, Williams, & Luckman, 2006). Unexpectedly, astrocyte activation of Astrocyte-ChR2 mice did not augment *c-fos* mRNA staining (Figure 3b). We quantified staining intensity for *c-fos* mRNA in the left and right cortex (blue and red rectangles in Figure 3a,b, respectively) by calculating their mean pixel values. While Neuron-ChR2 mice showed significantly higher staining for *c-fos* mRNA in the left cortex than that in the right cortex (107 ± 3 vs. 83 ± 7 in the left and right cortex, $p = .02$, $n = 9$ mice, paired t test; Figure 3a), Astrocyte-ChR2 mice showed comparable staining for *c-fos* mRNA in the left and right cortex (79 ± 6 vs. 79 ± 6 in the left and right cortex, $p = .86$, $n = 9$ mice, paired t test; Figure 3b).

This result cannot distinguish the following possibilities: (a) optogenetic activation of astrocytes indeed did not modulate neuronal activity or (b) it did modulate neuronal activity, but was not enough to increase expression of *c-fos* mRNA. To directly examine neuronal activity upon optogenetic stimulation of neurons or astrocytes, we next performed electrophysiological recording in the cortex of awake, head-fixed Neuron- or Astrocyte-ChR2 mice, using a linear 16-channel silicon probe electrode. This was a separate experiment to the ofMRI. Again, we observed neuronal activation upon optogenetic stimulation of Neuron-, but not of Astrocyte-ChR2 mice (Fig. 3c-f), supporting the first possibility.

Specifically, in Neuron-ChR2 mice, local field potential (LFP) power at the gamma and high frequency oscillation (HFO) significantly increased at the beginning of the stimulation, followed by a gradual decrease (Figure 3c). Average power of LFP at gamma and HFO during the period of the first light-activation was significantly higher than that during the pre-stimulus period (bar graph at lower right of Figure 3c; 6.3 ± 1.2 and 2.0 ± 0.6 for gamma and HFO; $p = .003$ and $.02$, respectively; $n = 6$ mice, paired t test). Multi-unit activities (MUA) in the cortex were also augmented by the optogenetic stimulation of Neuron-ChR2 mice (Figure 3e). The mean relative number of spikes during the first activation period (60~90 s) was significantly higher than that during the pre-stimulus period (lower panel of Figure 3e; 3.4 ± 0.6 , $p = .01$, $n = 6$ mice, paired t test). These results are in good accordance with previous reports (Kahn et al., 2013; Lee et al., 2010; Takata et al., 2015).

In Astrocyte-ChR2 mice, optogenetic activation of astrocytes did not modulate LFP power (Figure 3d). The average power of LFP during the first light activation period was not different from that during the pre-stimulus period (bar graph at lower right of Figure 3d; -0.2 ± 0.3 ,

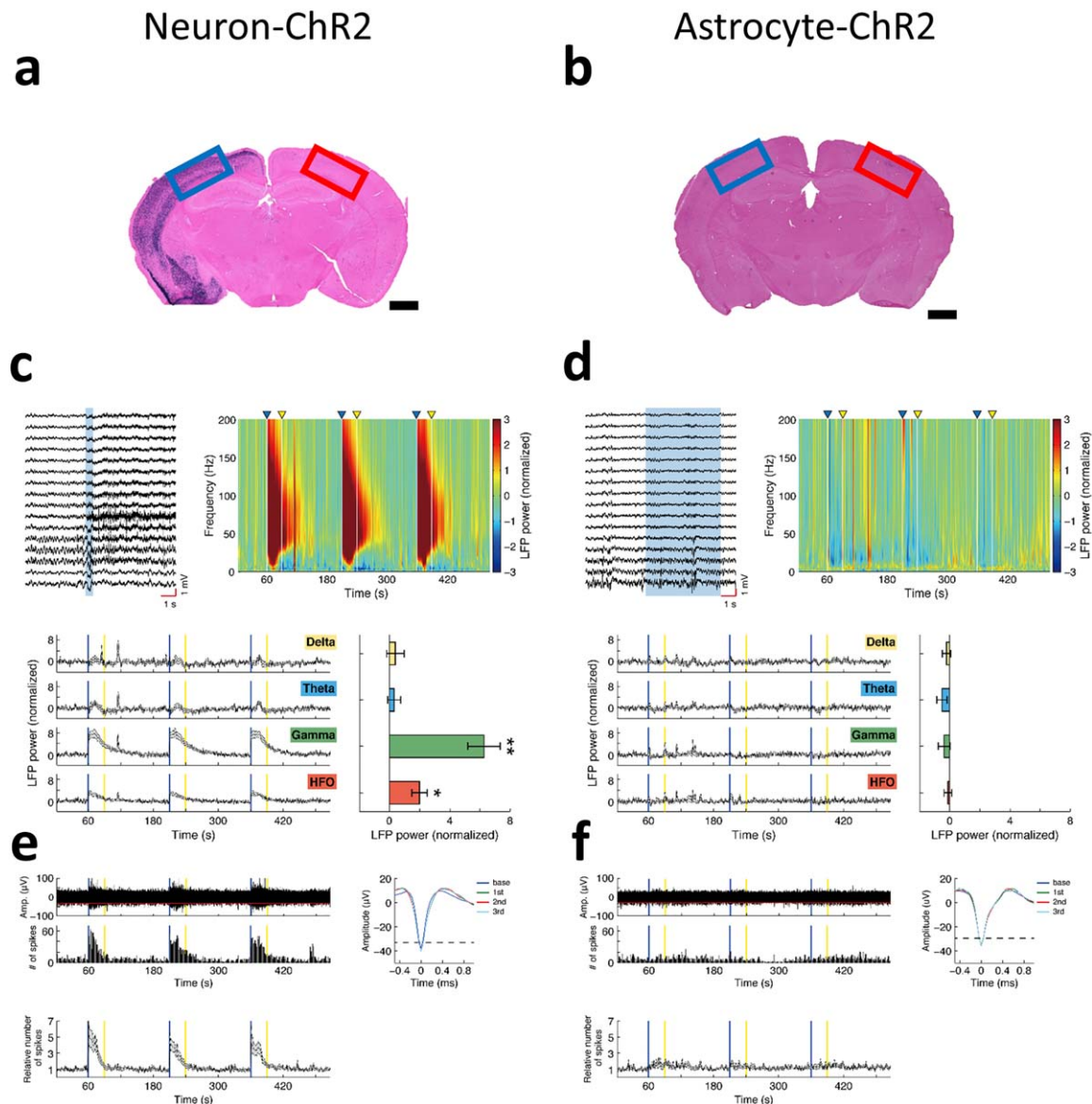


FIGURE 3 Optogenetic stimulation of neurons, but not astrocytes, results in neuronal activation. (a and b) Representative images of *in situ* hybridization on coronal brain sections around AP -2.0 mm for *c-fos* mRNA, 30 min after optogenetic stimulation of cortical neurons (a) or astrocytes (b) using Neuron- or Astrocyte-ChR2 mice, respectively ($n = 9$ each). Optogenetic stimulation of neurons, but not astrocytes, induced expression of *c-fos* mRNA (blue-purple signal) in the cortex ipsilateral to light illumination. Rectangles in blue and red were for quantification of staining intensity of *c-fos* mRNA. Scale bar: 1 mm. (c and d) LFP fluctuations upon optogenetic stimulation of Neuron- (c) or Astrocyte-ChR2 mice (d). Upper left: Representative traces of LFP recorded with a silicon probe electrode, inserted into the cortex of an awake Neuron- (c) or Astrocyte-ChR2 mouse (d). The blue area indicates the period of blue-light illumination. Note that the duration of light illumination was 0.5 and 5.0 s for Neuron- and Astrocyte-ChR2 mice, respectively. Upper right: Mean wavelet power spectrogram of LFP recorded in the cortex of $n = 6$ Neuron- (c) or $n = 5$ Astrocyte-ChR2 mice (d). Power values of LFP were normalized for each recording session. Blue and yellow triangles with white vertical lines indicate the delivery of blue and yellow light pulses, respectively. Lower left: Mean time courses of LFP-power at each frequency band. Vertical lines of blue and yellow indicate the delivery of light pulses of each color. The SEM envelopes the mean traces. Lower right: The bar graph compares the mean power of LFP at each frequency band during the first activation period (60~90 s). No modulation of LFP power was observed in Astrocyte-ChR2 mice (d). $*p < .05$, $**p < .01$; paired *t* test. (e and f) MUA response upon optogenetic stimulation of Neuron- (e) or Astrocyte-ChR2 mice (f). Upper left: A representative time course of high-pass filtered LFP (upper trace) and MUA (lower trace). A horizontal red line in the upper trace indicates a threshold for MUA extraction. Upper right: Representative mean traces of MUA during a baseline period (0~60 s, blue), and first (60~90 s, green), second (210~240 s, red), and third (360~390 s, pale blue) activation periods. Lower panel: Relative number of MUA counts, recorded from the most superficial 10 channels of the silicon probe in the cortex, from $n = 6$ Neuron- (e) and $n = 5$ Astrocyte-ChR2 mice (f). The SEM envelopes the mean traces [Color figure can be viewed at wileyonlinelibrary.com]

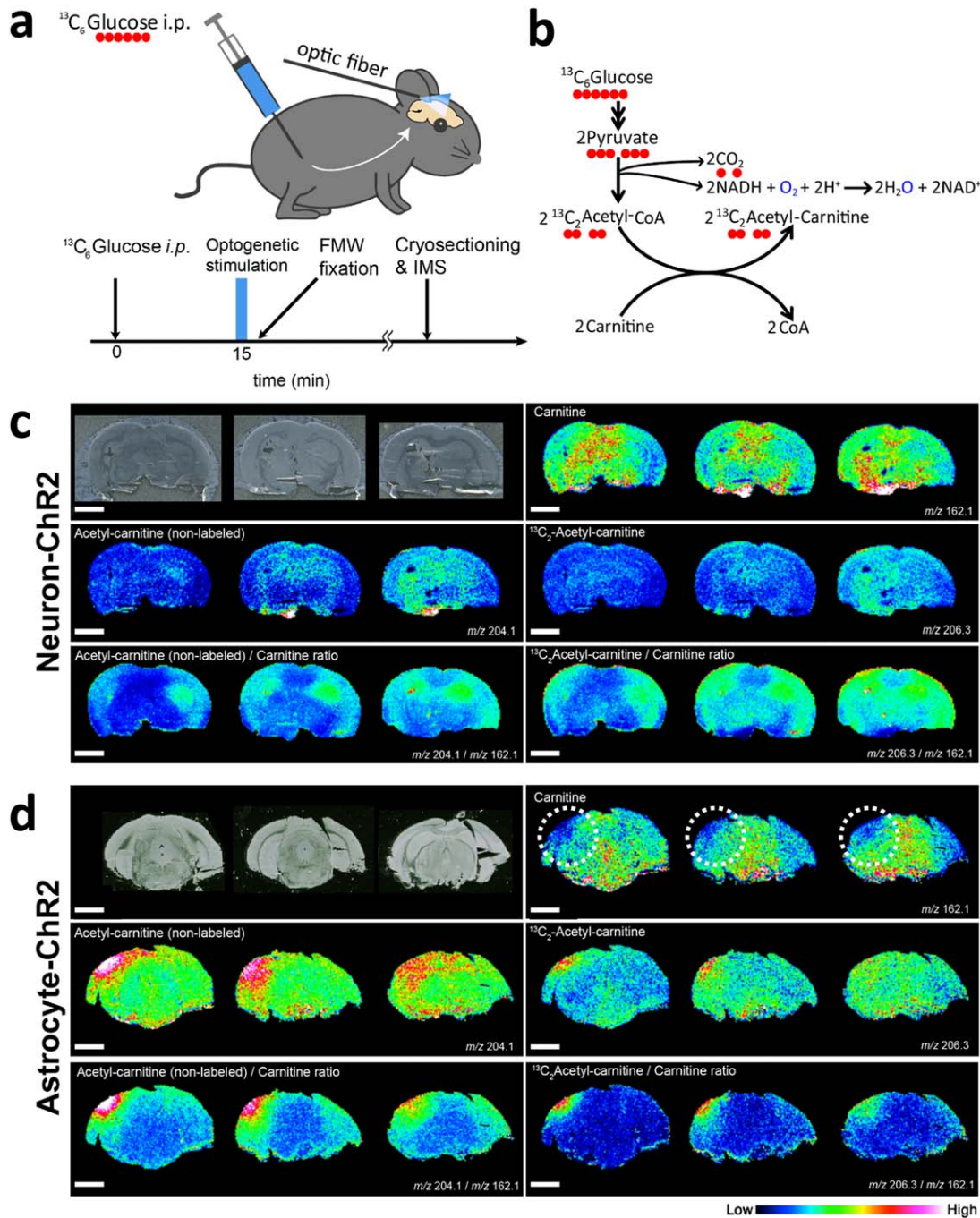


FIGURE 4 Synthesis of AC at the site of optogenetic activation of astrocytes, but not of neurons. (a) Upper panel: Schematic of IMS experiments, which involved pathway tracing of $^{13}\text{C}_6$ -labeled glucose upon optogenetic stimulation. A red circle indicates ^{13}C -isotope in a glucose molecule. Optic fiber was attached on the left intact skull. Lower panel: Experimental time course. FMW fixation of the brain was performed 30 s following optogenetic stimulation. (b) Schematic representation of $^{13}\text{C}_6$ -glucose metabolism into acetyl-carnitine (AC). (c and d) Representative IMS images for carnitine (right top), AC (left middle), $^{13}\text{C}_2$ -AC (middle right), AC/carnitine ratio (left bottom), and $^{13}\text{C}_2$ -AC/carnitine ratio (right bottom), after optogenetic stimulation of a Neuron- (c) or an Astrocyte-ChR2 mouse (d). Astrocyte activation augmented synthesis of AC that accompanies O_2 consumption (d, left middle). Upper left panel shows optical images of brain sections used for IMS. Each panel shows three consecutive slices. Dotted circles in a top right panel in (d) indicates area that showed reduction of carnitine. These experiments were repeated with $n = 3$ Neuron- and $n = 5$ Astrocyte-ChR2 mice, obtaining similar results. Scale bar: c and d, 2 mm [Color figure can be viewed at wileyonlinelibrary.com]

-0.5 ± 0.4 , -0.4 ± 0.4 , and -0.1 ± 0.3 for delta, theta, gamma, and HFO, respectively, $p > .25$, $n = 5$ mice, paired t test). Neither was MUA modulated (mean relative number of spikes during the first activation period: 1.3 ± 0.2 , $p = .22$, $n = 5$ mice, paired t test).

Illumination using only yellow light did not evoke electrophysiological response in Neuron- or Astrocyte-ChR2 mice (Supporting Information Figure S5a-d). The magnitude of electrophysiological response was dependent on intensities of blue light (Supporting Information



Figure S5e–h). These results were consistent with that of fMRI (Supporting Information Figure S3).

3.5 | $^{13}\text{C}_6$ -glucose is metabolized into $^{13}\text{C}_2$ -AC by optogenetic activation of astrocytes, but not neurons

We asked whether neuron- or astrocyte-evoked BOLD signal was underlain by the same metabolic activity because astrocyte-evoked BOLD signal accompanied oxygen consumption without neuronal activation (Figures 2 and 3). We used IMS to examine two-dimensional distribution of brain metabolites upon optogenetic stimulation of Neuron- or Astrocyte-ChR2 mice ($n = 3$ and 5 mice, respectively). Intraperitoneal injection of ^{13}C -isotope labeled glucose ($^{13}\text{C}_6$ -glucose) was performed fifteen minutes before optogenetic stimulation, which allowed us to trace flows of ^{13}C from glucose to various metabolites (Figure 4a,b). Transcranial light illumination for optogenetic stimulation of neurons or astrocytes was executed as before. Thirty seconds after the stimulation, was applied for 0.92 s to the head of the mouse to rapidly inactivate enzymatic reactions in the brain, which minimizes post-mortem alterations in metabolites during brain extraction (Sugiura et al., 2015). Brains were then extracted, frozen, and sliced coronally at a thickness of 8 μm . The spatial distribution of ^{13}C -containing metabolites that were synthesized from $^{13}\text{C}_6$ -glucose was explored and visualized using IMS.

Optogenetic stimulation of astrocytes, but not neurons, resulted in an increase of non-labeled AC and $^{13}\text{C}_2$ -AC at the site of light illumination in the cortex (Figure 4c,d, middle row), suggesting that AC was metabolized from glucose via oxidative decarboxylation of pyruvate to produce acetyl-CoA followed by transfer of acetyl-group to carnitine (Figure 4b). Concomitantly, reduction of carnitine, a substrate for AC synthesis, was observed at the same region in the brain of Astrocyte-ChR2 mice (dotted circles in Figure 4d, upper right panel), indicating that synthesis of AC from acetyl-CoA and carnitine occurred in the brain. Spatial patterns of fluctuation of these metabolites were similar to that of the BOLD signal response upon astrocyte activation (cf. Figure 2c with the bottom panels of Figure 4d or Supporting Information Figure S6a), implying that astrocyte activation accelerated the metabolic pathway that produces AC in the brain. Notably, optogenetic stimulation of astrocytes did not result in accumulation of NADH (Supporting Information Figure S6b, upper right panel). This suggests the presence of oxidative conversion of NADH to NAD^+ by mitochondrial complex I activity (Figure 4b). These imaging results were also supported by a capillary electrophoresis (CE)-electrospray ionization (ESI)-mass spectrometry (MS) technique (Morikawa et al., 2012; Sugiura et al., 2016; Supporting Information Figure S7). Taken together, these results suggest that while comparable a BOLD signal response was evoked by optogenetic stimulation of either neurons or astrocytes, the respective BOLD signal fluctuations were accompanied by distinct metabolic flows.

4 | DISCUSSION

We demonstrated that (a) selective stimulation of astrocytes is sufficient for the induction of a BOLD signal response with oxygen

consumption in the absence of neuronal activation, and (b) activation of astrocytes, but not neurons, resulted in glucose oxidation with production of AC, which is known to modulate neuronal energy processes (Pettegrew, Levine, & McClure, 2000; Traina, 2016). Our data present a causal relationship between astrocyte activation and BOLD signal generation, suggesting that BOLD signal fluctuations can reflect metabolic demands of astrocytes in addition to neurons. These findings may challenge the current interpretation of the BOLD signal response as a surrogate marker of neuronal activation in fMRI studies (Figley & Stroman, 2011; Gurden, 2013).

The physiological relevance of optogenetic stimulation of astrocytes has not been resolved completely, while increasingly many studies have recently employed optogenetic manipulation of astrocytes to utilize its advantages to shift the states of astrocytes non-invasively with cell-type specificity (Figueiredo et al., 2014; Gourine et al., 2010; Masamoto et al., 2015; Pelluru, Konadhode, Bhat, & Shiromani, 2016; Perea, Yang, Boyden, & Sur, 2014; Sasaki et al., 2012; Tanaka et al., 2012; Tang et al., 2014). The responses of astrocytes upon optogenetic activation have been reported as a few mV of depolarization, pH decrease, and cytosolic Ca^{2+} surge (Beppu et al., 2014; Perea et al., 2014; Sasaki et al., 2012), which can be observed in physiological situations (MacVicar, Crichton, Burnard, & Tse, 1987; Rose & Ransom, 1996; Seigneur, Kroeger, Nita, & Amzica, 2006; Takata et al., 2011).

Among the above three responses, depolarization of astrocytes might be the primary cause for BOLD signal induction in the current study, because we reported previously that astrocytic depolarization was coupled to efflux of potassium ions, a potent vasodilator, from astrocytes (Masamoto et al., 2015; Sasaki et al., 2012). Although we have shown that only ~ 5 mV depolarization was evoked with significantly larger light power (7 mW/mm² blue light illumination for 10 s; see Supporting Information Materials and Methods) on Bergmann glial cells (astrocytes in the cerebellum) in slice preparation from young Astrocyte-ChR2 mice (postnatal day 17–24), we have also demonstrated that amplitude of optogenetically induced inward currents developed age-dependent manner (Sasaki et al., 2012), suggesting that effect of optogenetic stimulation is larger in the current study that uses adult Astrocyte-ChR2 mice.

In the current study, optogenetic stimulation of astrocytes did not significantly activate neurons, which may appear inconsistent with previous reports that showed induction of *c-fos* mRNA in neuronal and/or glial cells upon optogenetic activation of astrocytes in the cortex or cerebellum using Astrocyte-ChR2 mice (Sasaki et al., 2012; Tanaka et al., 2012). While light intensity at the tip of the optic fiber was comparable among studies, the layout of the optic fiber differed: earlier studies placed an optic fiber perpendicular to the cranial skull, while the fiber was placed horizontally in the present study. Thus, it is conceivable that less light reached the brain in the current study, which may explain the lack of modulation of neuronal activity upon optogenetic manipulation of astrocytes. In line with this, astrocytes show distinct physiological response depending on stimulation intensity (Sekiguchi et al., 2016). It is possible that previous studies employed light illumination that was strong enough to modulate neuronal activity, because most of the studies used neuronal response as a readout for

optogenetic manipulation of astrocytes. It should be noted, however, that axonal activity cannot be detected with our extracellular electrodes. Therefore, the current study cannot exclude a possibility that optogenetic manipulation of astrocytes might have modulated axonal activity (Tang et al., 2014), which may lead to BOLD signal generation. Note that even in this case, our results support the idea of causal involvement of astrocytes in BOLD signal generation.

Optogenetic stimulation of astrocytes resulted in unexpected oxygen consumption without neuronal activation. We have previously shown that optogenetic activation of astrocytes results in potassium efflux from astrocytes (Masamoto et al., 2015), which should be followed by restoration of the ionic gradient of astrocytes by Na^+/K^+ -ATPase. Thus, synthesis of adenosine triphosphate (ATP) might be a candidate to account for the oxygen consumption, although we did not observe a significant increase in ATP upon optogenetic stimulation of astrocytes (Supporting Information Figure S6). AC might be another candidate for oxygen consumption upon optogenetic astrocyte activation, because metabolism from glucose to AC involves production of NADH, an electron donor that transfers an electron to molecular oxygen during oxidative phosphorylation in mitochondria (Figure 4b). In accord with this idea, NADH was not accumulated (Supporting Information Figure S6) while AC synthesis was evident (Figure 4d) upon optogenetic stimulation of astrocytes, suggesting consumption of a molecular oxygen by oxidization of NADH to NAD^+ in mitochondria (Figure 4b). See Supporting Information Discussion on the possibility of AC as an energy substrate for neurons.

The BOLD signal response has been used to infer activation of neurons because accumulating evidence has shown a close correlation between BOLD signal fluctuations and electrophysiological activation of neurons (Logothetis et al., 2001; Niessing et al., 2005). However, in the present study, we demonstrated that astrocytes can evoke a BOLD signal response that accompanies oxygen consumption without activation of local neurons. This may suggest the existence of BOLD signal fluctuations that are irrelevant to activation of local neurons. Indeed, a recent study found unexpected BOLD signal fluctuations that occurred without activation of local neurons during a repeated anticipation task (Sirotin & Das, 2009). Activation of astrocytes might be a cellular substrate underlying this type of BOLD signal fluctuation. What physiological mechanism might stimulate astrocytes without activation of local neurons? One possibility might be the release of neuromodulator(s) from axonal fibers of distant origin. It's shown that astrocytes are sensitive to neuromodulators such as acetylcholine and noradrenalin, which can be released in the cortex by axonal fibers ascending from the Meynert nucleus or Locus coeruleus, respectively (Bekar, He, & Nedergaard, 2008; Pankratov & Lalo, 2015; Takata et al., 2011). Thus, astrocytes may be able to respond to neuromodulatory activity of remote neurons, by augmenting metabolic activity including synthesis of AC that can be used as preparatory energy fuel for local neurons.

ACKNOWLEDGMENT

We thank Dr. Kouichi C. Nakamura for a generous gift of an antibody. We also thank Dr. Youcef Bouchekioua for his technical

support. This work was supported by Takeda Science Foundation to N.T.; JSPS KAKENHI Grant Numbers (25430011, 25115726, 15KT0111, 16H01620, and 16K07032 to N.T., 24111551 and 26290021 to K.F.T., 16H06145 to Y.S.); Brain/MINDS and the Strategic Research Program for Brain Sciences (SRPBS) from the Ministry of Education, Culture, Sports, Science, and Technology of Japan (MEXT) and Japan Agency for Medical Research and Development (AMED) to N.T., K.F.T. and H.O.

ORCID

Norio Takata  <http://orcid.org/0000-0003-2754-8562>

REFERENCES

- Aguado, F., Espinosa-Parrilla, J. F., Carmona, M. A., & Soriano, E. (2002). Neuronal activity regulates correlated network properties of spontaneous calcium transients in astrocytes in situ. *The Journal of Neuroscience*, 22(21), 9430–9444.
- Bekar, L. K., He, W., & Nedergaard, M. (2008). Locus coeruleus alpha-adrenergic-mediated activation of cortical astrocytes in vivo. *Cerebral Cortex*, 18(12), 2789–2795. <https://doi.org/10.1093/cercor/bhn040>
- Beppu, K., Sasaki, T., Tanaka, K. F., Yamanaka, A., Fukazawa, Y., Shigemoto, R., & Matsui, K. (2014). Optogenetic countering of glial acidosis suppresses glial glutamate release and ischemic brain damage. *Neuron*, 81(2), 314–320. <https://doi.org/10.1016/j.neuron.2013.11.011>
- Berndt, A., Yizhar, O., Gunaydin, L. A., Hegemann, P., & Deisseroth, K. (2009). Bi-stable neural state switches. *Nature Neuroscience*, 12(2), 229–234. <https://doi.org/10.1038/nn.2247>
- Ekstrom, A. (2010). How and when the fMRI BOLD signal relates to underlying neural activity: The danger in dissociation. *Brain Research Reviews*, 62(2), 233–244. <https://doi.org/10.1016/j.brainresrev.2009.12.004>
- Figley, C. R., & Stroman, P. W. (2011). The role(s) of astrocytes and astrocyte activity in neurometabolism, neurovascular coupling, and the production of functional neuroimaging signals. *The European Journal of Neuroscience*, 33(4), 577–588. <https://doi.org/10.1111/j.1460-9568.2010.07584.x>
- Figueiredo, M., Lane, S., Stout, R. F., Liu, B., Parpura, V., Teschemacher, A. G., & Kasparov, S. (2014). Comparative analysis of optogenetic actuators in cultured astrocytes. *Cell Calcium*, 56(3), 208–214. <https://doi.org/10.1016/j.ceca.2014.07.007>
- Gourine, A. V., Kasymov, V., Marina, N., Tang, F., Figueiredo, M. F., Lane, S., ... Kasparov, S. (2010). Astrocytes control breathing through pH-dependent release of ATP. *Science*, 329(5991), 571–575. <https://doi.org/10.1126/science.1190721>
- Greenberg, D. S., Houweling, A. R., & Kerr, J. N. D. (2008). Population imaging of ongoing neuronal activity in the visual cortex of awake rats. *Nature Neuroscience*, 11(7), 749–751. <https://doi.org/10.1038/nn.2140>
- Gurden, H. (2013). Astrocytes: Can they be the missing stars linking neuronal activity to neurofunctional imaging signals? *Frontiers in Cellular Neuroscience*, 7, 21. <https://doi.org/10.3389/fncel.2013.00021>
- Haydon, P. G., & Carmignoto, G. (2006). Astrocyte control of synaptic transmission and neurovascular coupling. *Physiological Reviews*, 86(3), 1009–1031. <https://doi.org/10.1152/physrev.00049.2005>
- Heeger, D. J., & Ress, D. (2002). What does fMRI tell us about neuronal activity? *Nature Reviews Neuroscience*, 3(2), 142–151. <https://doi.org/10.1038/nrn730>

- Jego, P., Pacheco-Torres, J., Araque, A., & Canals, S. (2014). Functional MRI in mice lacking IP3-dependent calcium signaling in astrocytes. *Journal of Cerebral Blood Flow & Metabolism*, 34(10), 1599–1603. <https://doi.org/10.1038/jcbfm.2014.144>
- Kahn, I., Knoblich, U., Desai, M., Bernstein, J., Graybiel, A. M., Boyden, E. S., ... Moore, C. I. (2013). Optogenetic drive of neocortical pyramidal neurons generates fMRI signals that are correlated with spiking activity. *Brain Research*, 1511, 33–45. <https://doi.org/10.1016/j.brainres.2013.03.011>
- Lee, J. H., Durand, R., Gradinaru, V., Zhang, F., Goshen, I., Kim, D.-S., ... Deisseroth, K. (2010). Global and local fMRI signals driven by neurons defined optogenetically by type and wiring. *Nature*, 465(7299), 788–792. <https://doi.org/10.1038/nature09108>
- Logothetis, N. K., Pauls, J., Augath, M., Trinath, T., & Oeltermann, A. (2001). Neurophysiological investigation of the basis of the fMRI signal. *Nature*, 412(6843), 150–157. <https://doi.org/10.1038/35084005>
- MacVicar, B. A., Crichton, S. A., Burnard, D. M., & Tse, F. W. (1987). Membrane conductance oscillations in astrocytes induced by phorbol ester. *Nature*, 329(6136), 242–243. <https://doi.org/10.1038/329242a0>
- Maier, A., Wilke, M., Aura, C., Zhu, C., Ye, F. Q., & Leopold, D. A. (2008). Divergence of fMRI and neural signals in V1 during perceptual suppression in the awake monkey. *Nature Neuroscience*, 11(10), 1193–1200. <https://doi.org/10.1038/nn.2173>
- Masamoto, K., & Kanno, I. (2012). Anesthesia and the quantitative evaluation of neurovascular coupling. *Journal of Cerebral Blood Flow & Metabolism*, 32(7), 1233–1247. <https://doi.org/10.1038/jcbfm.2012.50>
- Masamoto, K., Unekawa, M., Watanabe, T., Toriumi, H., Takuwa, H., Kawaguchi, H., ... Suzuki, N. (2015). Unveiling astrocytic control of cerebral blood flow with optogenetics. *Scientific Reports*, 5(1), 11455. <https://doi.org/10.1038/srep11455>
- Mattis, J., Tye, K. M., Ferenczi, E. A., Ramakrishnan, C., O'Shea, D. J., Prakash, R., ... Deisseroth, K. (2012). Principles for applying optogenetic tools derived from direct comparative analysis of microbial opsins. *Nature Methods*, 9(2), 159–172. <https://doi.org/10.1038/nmeth.1808>
- Mishra, A., Reynolds, J. P., Chen, Y., Gourine, A. V., Rusakov, D. A., & Attwell, D. (2016). Astrocytes mediate neurovascular signaling to capillary pericytes but not to arterioles. *Nature Neuroscience*, 19(12), 1619–1627. <https://doi.org/10.1038/nn.4428>
- Morikawa, T., Kajimura, M., Nakamura, T., Hishiki, T., Nakanishi, T., Yukutake, Y., ... Suematsu, M. (2012). Hypoxic regulation of the cerebral microcirculation is mediated by a carbon monoxide-sensitive hydrogen sulfide pathway. *Proceedings of the National Academy of Sciences*, 109(4), 1293–1298. <https://doi.org/10.1073/pnas.1119658109>
- Nagaoka, T., Zhao, F., Wang, P., Harel, N., Kennan, R. P., Ogawa, S., & Kim, S.-G. (2006). Increases in oxygen consumption without cerebral blood volume change during visual stimulation under hypotension condition. *Journal of Cerebral Blood Flow & Metabolism*, 26(8), 1043–1051. <https://doi.org/10.1038/sj.jcbfm.9600251>
- Niessing, J., Ebisch, B., Schmidt, K. E., Niessing, M., Singer, W., & Galuske, R. A. W. (2005). Hemodynamic signals correlate tightly with synchronized gamma oscillations. *Science (New York, N.Y.)*, 309(5736), 948–951. <https://doi.org/10.1126/science.1110948>
- Ogawa, S., Lee, T. M., Kay, A. R., & Tank, D. W. (1990). Brain magnetic resonance imaging with contrast dependent on blood oxygenation. *Proceedings of the National Academy of Sciences of the United States of America*, 87(24), 9868–9872.
- Ogawa, S., Menon, R. S., Kim, S. G., & Ugurbil, K. (1998). On the characteristics of functional magnetic resonance imaging of the brain. *Annual Review of Biophysics and Biomolecular Structure*, 27(1), 447–474. <https://doi.org/10.1146/annurev.biophys.27.1.447>
- Otsu, Y., Couchman, K., Lyons, D. G., Collot, M., Agarwal, A., Mallet, J.-M., ... Charpak, S. (2015). Calcium dynamics in astrocyte processes during neurovascular coupling. *Nature Neuroscience*, 18(2), 210–218. <https://doi.org/10.1038/nn.3906>
- Pankratov, Y., & Lalo, U. (2015). Role for astroglial α 1-adrenoreceptors in gliotransmission and control of synaptic plasticity in the neocortex. *Frontiers in Cellular Neuroscience*, 9, 230. <https://doi.org/10.3389/fncel.2015.00230>
- Pelluru, D., Konadhode, R. R., Bhat, N. R., & Shiromani, P. J. (2016). Optogenetic stimulation of astrocytes in the posterior hypothalamus increases sleep at night in C57BL/6J mice. *European Journal of Neuroscience*, 43(10), 1298–1306. <https://doi.org/10.1111/ejn.13074>
- Perea, G., Yang, A., Boyden, E. S., & Sur, M. (2014). Optogenetic astrocyte activation modulates response selectivity of visual cortex neurons in vivo. *Nature Communications*, 5, <https://doi.org/10.1038/ncomms4262>
- Pettegrew, J. W., Levine, J., & McClure, R. J. (2000). Acetyl-L-carnitine physical-chemical, metabolic, and therapeutic properties: Relevance for its mode of action in Alzheimer's disease and geriatric depression. *Molecular Psychiatry*, 5(6), 616–632.
- Petzold, G. C., & Murthy, V. N. (2011). Role of astrocytes in neurovascular coupling. *Neuron*, 71(5), 782–797. <https://doi.org/10.1016/j.neuron.2011.08.009>
- Raichle, M. E., & Mintun, M. A. (2006). Brain work and brain imaging. *Annual Review of Neuroscience*, 29(1), 449–476. <https://doi.org/10.1146/annurev.neuro.29.051605.112819>
- Rose, C. R., & Ransom, B. R. (1996). Mechanisms of H⁺ and Na⁺ changes induced by glutamate, kainate, and d-aspartate in rat hippocampal astrocytes. *The Journal of Neuroscience*, 16(17), 5393–5404.
- Sasaki, T., Beppu, K., Tanaka, K. F., Fukazawa, Y., Shigemoto, R., & Matsui, K. (2012). Application of an optogenetic byway for perturbing neuronal activity via glial photostimulation. *Proceedings of the National Academy of Sciences of the United States of America*, 109(50), 20720–20725. <https://doi.org/10.1073/pnas.1213458109>
- Schulz, K., Sydekum, E., Krueppel, R., Engelbrecht, C. J., Schlegel, F., Schröter, A., ... Helmchen, F. (2012). Simultaneous BOLD fMRI and fiber-optic calcium recording in rat neocortex. *Nature Methods*, 9(6), 597–602. <https://doi.org/10.1038/nmeth.2013>
- Schummers, J., Yu, H., & Sur, M. (2008). Tuned responses of astrocytes and their influence on hemodynamic signals in the visual cortex. *Science*, 320(5883), 1638–1643. <https://doi.org/10.1126/science.1156120>
- Seigneur, J., Kroeger, D., Nita, D. A., & Amzica, F. (2006). Cholinergic action on cortical glial cells in vivo. *Cerebral Cortex*, 16(5), 655–668. <https://doi.org/10.1093/cercor/bhj011>
- Sekiguchi, K. J., Shekhtmeyster, P., Merten, K., Arena, A., Cook, D., Hoffman, E., ... Nimmerjahn, A. (2016). Imaging large-scale cellular activity in spinal cord of freely behaving mice. *Nature Communications*, 7, 11450. <https://doi.org/10.1038/ncomms11450>
- Shen, Q., Ren, H., & Duong, T. Q. (2008). CBF, BOLD, CBV, and CMRO2 fMRI signal temporal dynamics at 500-msec resolution. *Journal of Magnetic Resonance Imaging*, 27(3), 599–606. <https://doi.org/10.1002/jmri.21203>
- Sirotnin, Y. B., & Das, A. (2009). Anticipatory haemodynamic signals in sensory cortex not predicted by local neuronal activity. *Nature*, 457(7228), 475–479. <https://doi.org/10.1038/nature07664>
- Sokoloff, L., Reivich, M., Kennedy, C., Rosiers, M. H. D., Patlak, C. S., Pettigrew, K. D., ... Shinohara, M. (1977). The [¹⁴C]deoxyglucose method for the measurement of local cerebral glucose utilization:

- Theory, procedure, and normal values in the conscious and anesthetized albino rat. *Journal of Neurochemistry*, 28(5), 897–916. <https://doi.org/10.1111/j.1471-4159.1977.tb10649.x>
- Srinivasan, R., Huang, B. S., Venugopal, S., Johnston, A. D., Chai, H., Zeng, H., ... Khakh, B. S. (2015). Ca²⁺ signaling in astrocytes from Ip3r2^{-/-} mice in brain slices and during startle responses in vivo. *Nature Neuroscience*, 18(5), 708–717. <https://doi.org/10.1038/nn.4001>
- Stark, J. A., Davies, K. E., Williams, S. R., & Luckman, S. M. (2006). Functional magnetic resonance imaging and c-Fos mapping in rats following an anorectic dose of m-chlorophenylpiperazine. *NeuroImage*, 31(3), 1228–1237. <https://doi.org/10.1016/j.neuroimage.2006.01.046>
- Stobart, J. L., Ferrari, K. D., Barrett, M. J. P., Stobart, M. J., Looser, Z. J., Saab, A. S., & Weber, B. (2016). Long-term in vivo calcium imaging of astrocytes reveals distinct cellular compartment responses to sensory stimulation. *Cerebral Cortex*, 28(1), 184–198. <https://doi.org/10.1093/cercor/bhw366>
- Sugiura, Y., Honda, K., Kajimura, M., & Suematsu, M. (2014). Visualization and quantification of cerebral metabolic fluxes of glucose in awake mice. *Proteomics*, 14(7–8), 829–838. <https://doi.org/10.1002/pmic.201300047>
- Sugiura, Y., Honda, K., & Suematsu, M. (2015). Development of an imaging mass spectrometry technique for visualizing localized cellular signaling mediators in tissues. *Mass Spectrometry*, 4(1), A0040–A0049. <https://doi.org/10.5702/massspectrometry.A0040>
- Sugiura, Y., Katsumata, Y., Sano, M., Honda, K., Kajimura, M., Fukuda, K., & Suematsu, M. (2016). Visualization of in vivo metabolic flows reveals accelerated utilization of glucose and lactate in penumbra of ischemic heart. *Scientific Reports*, 6(1), 32361. <https://doi.org/10.1038/srep32361>
- Sugiura, Y., Taguchi, R., & Setou, M. (2011). Visualization of spatiotemporal energy dynamics of hippocampal neurons by mass spectrometry during a kainate-induced seizure. *PLoS One*, 6(3), e17952. <https://doi.org/10.1371/journal.pone.0017952>
- Takano, T., Tian, G.-F., Peng, W., Lou, N., Libionka, W., Han, X., & Nedergaard, M. (2006). Astrocyte-mediated control of cerebral blood flow. *Nature Neuroscience*, 9(2), 260–267. <https://doi.org/10.1038/nn1623>
- Takata, N., Mishima, T., Hisatsune, C., Nagai, T., Ebisui, E., Mikoshiba, K., & Hirase, H. (2011). Astrocyte calcium signaling transforms cholinergic modulation to cortical plasticity in vivo. *The Journal of Neuroscience*, 31(49), 18155–18165. <https://doi.org/10.1523/JNEUROSCI.5289-11.2011>
- Takata, N., Yoshida, K., Komaki, Y., Xu, M., Sakai, Y., Hikishima, K., ... Tanaka, K. F. (2015). Optogenetic activation of CA1 pyramidal neurons at the dorsal and ventral hippocampus evokes distinct brain-wide responses revealed by mouse fMRI. *PLoS One*, 10(3), e0121417. <https://doi.org/10.1371/journal.pone.0121417>
- Tanaka, K. F., Matsui, K. O., Sasaki, T., Sano, H., Sugio, S., Fan, K., ... Yamanaka, A. (2012). Expanding the repertoire of optogenetically targeted cells with an enhanced gene expression system. *Cell Reports*, 2(2), 397–406. <https://doi.org/10.1016/j.celrep.2012.06.011>
- Tang, F., Lane, S., Korsak, A., Paton, J. F. R., Gourine, A. V., Kasparov, S., & Teschemacher, A. G. (2014). Lactate-mediated glianeuronal signaling in the mammalian brain. *Nature Communications*, 5, 3284. <https://doi.org/10.1038/ncomms4284>
- Thrane, A. S., Thrane, V. R., Zeppenfeld, D., Lou, N., Xu, Q., Nagelhus, E. A., & Nedergaard, M. (2012). General anesthesia selectively disrupts astrocyte calcium signaling in the awake mouse cortex. *Proceedings of the National Academy of Sciences of the United States of America*, 109(46), 18974–18979. <https://doi.org/10.1073/pnas.1209448109>
- Traina, G. (2016). The neurobiology of acetyl-L-carnitine. *Frontiers in Bioscience (Landmark Edition)*, 21, 1314–1329.
- Tsurugizawa, T., Ciobanu, L., & Le Bihan, D. (2013). Water diffusion in brain cortex closely tracks underlying neuronal activity. *Proceedings of the National Academy of Sciences of the United States of America*, <https://doi.org/10.1073/pnas.1303178110>
- Vanzetta, I., & Sloviter, H. (2010). A BOLD assumption. *Frontiers in Neuroenergetics*, 2, <https://doi.org/10.3389/fnene.2010.00024>
- Yoshida, K., Mimura, Y., Ishihara, R., Nishida, H., Komaki, Y., Minakuchi, T., ... Takata, N. (2016). Physiological effects of a habituation procedure for functional MRI in awake mice using a cryogenic radiofrequency probe. *Journal of Neuroscience Methods*, 274, 38–48. <https://doi.org/10.1016/j.jneumeth.2016.09.013>

SUPPORTING INFORMATION

Additional Supporting Information may be found online in the supporting information tab for this article.

How to cite this article: Takata N, Sugiura Y, Yoshida K, et al. Optogenetic astrocyte activation evokes BOLD fMRI response with oxygen consumption without neuronal activity modulation. *Glia*. 2018;00:1–11. <https://doi.org/10.1002/glia.23454>